Wetter environment and increased grazing reduced the area burned in northern Eurasia: 2002 – 2016

Wei Min Hao[1], Matthew C. Reeves[2], L. Scott Baggett[3], Yves Balkanski[4], Philippe Ciais[4], Bryce L. Nordgren[1], Alexander Petkov[1], Rachel E. Corley[1], Florent Mouillot[5], Shawn P. Urbanski[1], Chao Yue[6]

[1]United States Forest Service, Rocky Mountain Research Station, Fire Sciences Laboratory, 5775 Highway 10 West, Missoula, MT 59808 USA.
[2]United States Forest Service, Rocky Mountain Research Station, Forestry Sciences Laboratory, 800 E. Beckwith, Missoula, MT 59801, USA.
[3]United States Forest Service, Rocky Mountain Research Station, 240 West Prospect, Fort Collins, CO 80526, USA.
[4]Laboratoire des Sciences du Climat et de l'Environnement, LSCE CEA CNRS UVSQ, 91191 Gif Sur Yvette, France.
[5]UMR CEFE 5175, Centre National de la Recherche Scientifique (CNRS), Université de Montpellier, Université Paul-Valéry Montpellier, Ecole Pratique des Hautes Etudes (EPHE), Institut de Recherche pour le Développement, 34293 Montpellier CEDEX 5, France.
[6]Institute of Soil and Water Conservation, Northwest A&F University, Yangling, Shaanxi 712100, P.R. China.

Correspondence: Wei Min Hao (weimin.hao@usda.gov)

Abstract. Northern Eurasia is highly sensitive to climate change. Fires in this region can have significant impacts on regional air quality, radiative forcing and black carbon deposition in the Arctic to accelerate ice melting. Using a MODIS-derived burned area data set, we report that the total annual area burned in this region declined by 53 % during the 15-year period of 2002–2016. Grassland fires dominated the trend, accounting for 93 % of the decline of the total area burned. Grassland fires in Kazakhstan contributed 47 % of the total area burned and 84% of the decline. Wetter climate and increased grazing are the principle driving forces for the decline. Our findings: 1) highlight the importance of the complex interactions of climate-vegetation-land use in affecting fire activity, and 2) reveal how the resulting impacts on fire activity in a relatively small region such as Kazakhstan can dominate the trends of burned areas across a much larger landscape of northern Eurasia. Our findings may be used to improve the prediction of future fire dynamics and associated fire emissions in northern Eurasia.

1 Introduction

Fire activity worldwide is very sensitive to climate change and human actions, especially over high latitude ecosystems (Goetz et al., 2007). Identifying and unraveling confounding fire drivers is critical for understanding the recent and future impacts of fire activity. In northern Eurasia fire activity impacts of chief concern include carbon cycling, boreal ecosystem dynamics, fire emissions (Hao et al., 2016a), accelerated ice melting in the Arctic (Hao et al., 2016a; Evangeliou et al., 2016), early thawing of permafrost, the hydrological cycle of high-latitudes (IPCC, 2014), and air quality in Europe, Asia and North America. An improved understanding of the region's fire dynamics can also be applied to develop climate change mitigation policy and be incorporated into the fire modules of Earth System Models to improve their predictions (Hantson et al. 2016).

Global mean surface temperature rose by approximately 0.72° C from the year 1951 to 2012 according to the 5th Intergovernmental Panel on Climate Change Report (IPCC) (IPCC, 2013), but remained relatively constant ("warming hiatus") from 1998 to 2013 (Fyfe et al., 2013; Cowtan and Way, 2014; Trenberth et al., 2014). Nevertheless, extreme high temperature events continued to occur even during the warming hiatus (Seneviratne et al., 2014; Trenberth et al., 2015). Since 2013, the global temperatures have risen rapidly (NASA Global Climate Change, 2019). High latitudes are projected to have the largest temperature increase globally by 2100 (IPCC, 2013). At the same time, however, components of the fire weather index (FWI), an index of fire intensity potential, have experienced regional divergence at these latitudes with a positive FWI trend in Eastern Asia and a negative trend in Kazakhstan (Jolly et al. 2015), suggesting divergent regional climate impacts.

Northern Eurasia, defined here as a region from 35° N to the Arctic and from the Pacific Ocean to the Atlantic Ocean, comprises 21 % of the Earth's land area and encompasses diverse ecosystems from the steppes of central Asia to the Arctic. Forest is the major ecosystem covering an area of 27 % in northern Eurasia (Friedl et al., 2010), followed by grassland of 16 %. Over the past 20 years, the decline of total area burned in Eurasia has been observed by Giglio et al., 2013; Hao et al., 2016a and Andela et al., 2017.

Fire activity is greatly influenced by climate, fuels and human activity in different ways over different ecosystems (e.g. Pausas and Ribeiro, 2013; Andela et al., 2017). Considerable research has been done to understand climate-fire-grazing interactions in grassland ecosystems. In grasslands reductions in fuel availability due to decreasing net primary production, grazing, or other management activities can be the key variables limiting fire spread (Moritz et al., 2005). In the western United States, the research has significant implications on forest and rangeland management (e.g. Bachelet et al., 2000; Gedalof et al., 2005; Riley et al., 2013; Abatzoglou and Kolden, 2013). Similar issues were investigated on African savanna for maintaining sustainable grassland (e.g. Archibald et al., 2009; Koerner and Collins, 2014). In this study we closely examine the interactions of climate, fire, grazing and fuel availability in the region of northern Eurasia with the largest decline in burned area during 2002–2016.

To disentangle keystone variables affecting fire activity, we examined the trends of the spatial and temporal distribution of the area burned from 2002 to 2016 across different land cover types and geographic regions of northern Eurasia. Daily NASA MODIS (**Mod**erate Resolution **I**maging **S**pectroradiometer) dataset at a 500 m × 500 m resolution was used. The burned area data were analyzed at multiple spatial and temporal scales using frequentist statistical methods to identify the regional trends. We identified the geographic region with the largest declining trend and explore the influence of the confounding factors of climate and human activity on burned area in this region. Assessing burned area changes in northern Eurasia over this time period benefits from the lack of fire suppression in this region (Goldammer et al., 2013), so the impact of climate and land use on fire activity can be better understood.

2 Methodology

2.1 Mapping burned areas

Since the year 2000, global burned area has been mapped by remote sensing (e.g. Mouillot et al. 2014) with different sensors and detection algorithms (Chuvieco et al., 2019), leading to multiple datasets with a significant uncertainty in the magnitude of spatial distribution, interannual variability and trends in burned area (Hantson et al. 2016). Our methodology used for mapping daily burned area is very similar to that used by Hao et al. (2016a, 2016b), with the only difference being the land cover product. This study used annual edition of land cover/land cover change product (MCD12) for 2002–2013 and the land cover map for 2013 was used for the years of 2014–2016 because current versions were not available. The study of Hao et al. (2016a, 2016b) used the MCD12 land cover map of 2005 for all years. This study used the land cover map for collection 5 (Friedl et al., 2010) which was no longer available for download. The methodology has been validated in eastern Siberia (Hao et al., 2016a). The Forest Service Fire Emission Inventory – Northern Eurasia (FEI-NE) burned area dataset has been used to estimate black carbon emissions in northern Eurasia and their transport and deposition to the Arctic (Hao et al., 2016a; Evangeliou et al., 2016).

2.2 Data sources of drought, land cover and livestock

We will describe the data sources for estimating the factors affecting the burned area in Kazakhstan: drought, land cover, ecosystem productivity and livestock density. All data were evaluated at the county level for 174 counties during the period of 1992–2016 (Fig. 1). We focused on Kazakhstan as the region with the largest decline of burned area in northern Eurasia (see section 3.1).

Drought

The Palmer Drought Severity Index (PDSI) from the TerraClimate site (http://www.climatologylab.org/) was used to estimate drought throughout the study area. The PDSI was developed by Palmer (1965) and is widely used to estimate a rough soil water budget based on monthly precipitation, potential evapotranspiration with varying soil property of available water content to account for pedological variations and species roots access to water. Among the monthly PDSI values available, we used monthly PDSI data from March to July, defined as the fire season (Roy et al., 2008), to compute a cumulative drought effect index from March to July in 2002–2016. The gridded PDSI data were available at a spatial resolution of ~ 4 km and were aggregated to the 174 counties within the study area (Fig. 1). PDSI varies from +4 for wet conditions to -4 for dry conditions.

Livestock

The annual population of livestock in each of the 14 provinces of Kazakhstan from 2002 to 2016 were compiled by the official agriculture statistics of the Ministry of National Economy of the Republic of Kazakhstan Committee on Statistics (MANE 2019). These data included yearly numbers of large horned livestock and sheep and goats at the province level which is coarser than the counties. Livestock populations are only available at the province level and the population was distributed proportionally to the size of the county area so that all potential drivers of fire activity could be evaluated on a common spatial scale. The livestock density for each county is defined as the ratio of the number of animals to the size of the county.

Annual Biomass Production

We estimated the annual biomass production within the grassland domain of the study area (Fig. 2) using the production subroutine of the Rangeland Vegetation Simulator model (RVS) (Reeves 2016). The RVS, which was originally developed for simulating rangeland vegetation dynamics in the continental United States, models annual production based on MODIS normalized difference vegetation index (NDVI) at a 250 m spatial resolution (MOD13Q1). The MOD13Q1 NDVI data are composited on a bi-weekly basis and are available at a spatial resolution of 250 m. The QA/QC flags were used to isolate only the best quality NDVI pixels. The conversion of NDVI to aboveground net primary production (ANPP) for non-forest environments in the RVS is divided into two groups to enable different models to be fit to the lower and upper end of production given as

$$ANPP = 240.31 * e^{3.6684} (X) \qquad (1)$$

where estimated ANPP is in lbs ac^{-1} of dry weight and X is the annual maximum NDVI for the upper range ($X \geq 0.46$) and

$$ANPP = 971.1 * \ln (X) + 1976 \qquad (2)$$

where X is the annual maximum NDVI for the lower range ($X < 0.46$).

Land Cover

The MODIS land cover product (MOD12Q1) Version 6.0 was used to assess factors affecting the burned area in Kazakhstan. The product is available at a 500 m spatial resolution and describes the distribution of broad vegetation types. We screened these data to subset only those vegetation types considered to represent grassland vegetation (Class 10 in the MOD12Q1 dataset) from 2000 to 2016.

Statistical Analysis

For each pixel of 0.5° × 0.5°, the annual trend was estimated as the robust linear slope computed from burned area on year using M-estimation as described in Huber (1981). The trends were estimated using the R platform (R Core Team, 2019) with R function *rlm* in package MASS (Venables and Ripley, 2002). Pairwise robust rank correlations were computed as described in Kendall (1938) using the R function *cor*.

To validate our estimates on burned areas, we compare of our annual northern Eurasia burned areas (FEI-NE) with the latest version of the MODIS burned area product (MCD64A1, collection 6) (Gigilio et al., 2018) from 2002 to 2016. The burned areas reported by FEI-NE and MODIS MCD64 were each modeled separately by year. The models each include a first-order autoregressive term on the residuals to account for the presence of temporal autocorrelation. The response was assumed to be gamma distributed. A generalized linear mixed model (GLMM) approach was used and estimated using the R function *glmmTMB* in platform (R Core Team, 2019) with R package *glmmTMB* (Brooks et al., 2017).

The potential driving forces of burned area at the county level of 174 counties over a period of 15 years from 2002 to 2016 were modeled using frequentist to interpret the effects on the extent of the area burned. The proportion of burned area per county was modeled on the effects of year, PDSI during the fire season (May-July), proportion of grass area, ANPP and livestock density along with two-way interactions. The model included a random effect that accounts for spatial correlation within each region along with a first-order autoregressive term on the residuals within each county that accounts for temporal autocorrelation. The response was assumed to be beta distributed. A generalized linear mixed model (GLMM) approach was used and estimated using the R platform (R Core Team, 2019) with R package glmmTMB (Brooks et al., 2017).

3 Results

3.1 Spatial and temporal distribution of burned areas

The declining trends in the spatial distribution of the area burned from 2002 to 2016 in northern Eurasia at a 0.5° × 0.5° resolution are shown in Fig. 2. The majority of the area burned in the 15 years was grassland of Kazakhstan in central Asia. However, substantial areas were also burned in the Russian Far East along the Chinese border because of illegal logging (Vandergert and Newell, 2003) and the subsequent fires to burn the remaining forest residues. The annual areas burned according to ecosystem and geographic region are summarized in Table 1. The interannual burned area in northern Eurasia varied about four times within a range from 1.2×10^5 km^2 in 2013 to 5.0×10^5 km^2 in 2003 with an average of $(2.7 \pm 1.0) \times 10^5$ km^2 (n = 15). Grassland accounted for 71 % of the total area burned, despite comprising only 16 % of the land cover (Friedl et al., 2010). Almost all the grassland fires occurred in Kazakhstan in central and western Asia (Table 1). In contrast, forest is the major ecosystem that covers 27 % of northern Eurasia (Friedl et al., 2010), but contributes only 18 % of the total area burned. About ninety percent of the forest area burned occurred in Russia.

3.2 Trends of burned areas

Comparisons of our annual northern Eurasia burned areas (FEI-NE) with the latest version of the MODIS burned area product (MCD64A1, collection 6) (Gigilio et al., 2018) from 2002 to 2016 are shown in Fig. 3. The burned areas in these two datasets agree better in recent years after 2010. Both FEI-NE and MCD64A1 demonstrated declining trends and similar interannual variability. The FEI-NE dataset was used to analyze the driving forces for the decline of burned area in Kazakhstan (see sections 3.3–3.4).

Grasslands of Kazakhstan dominate the changes of the burned area with significant declines mostly in central and northern Kazakhstan, adjacent to the Russian border. The temporal trend of annual burned areas over all vegetation types and in grasslands in northern Eurasia and in Kazakhstan from 2002 to 2016 are shown in Fig. 4. The burned area trends shown in Fig. 4 were modeled like that reported in Fig. 3 with the same response distribution. The annual total area burned over northern Eurasia during this period decreased by 53 % from 3.3×10^5 km^2 in 2002 to

1.6×10^5 km^2 in 2016 (Table 1), or at a rate of 1.2×10^4 km^2 (or 3.5 %) yr^{-1}. The grassland area burned during the 15 years declined by 74 % from 2.8×10^5 km^2 in 2002 to 7.3×10^4 km^2 in 2016, or at a rate of 1.3×10^4 km^2 (or 4.9 %) yr^{-1}. Grassland fires in Kazakhstan accounted for 47 % of the total areas burned but contributed 84 % of the declining trend. The annual forest burned area varied by a factor of 5 from 21,243 km^{-2} in 2010 to 111,019 km^{-2} in 2003, but there is no trend over the 15 years (Table 1).

3.3 Regional trends in driving forces over time

One of our objectives was to evaluate trends in the primary drivers responsible for reducing area burned, especially in grasslands at the county level. Pairwise correlation results are shown in Fig. 5. Each panel of Fig. 5 illustrates the coefficient of correlation between a key variable and year (2002–2016) for the 174 counties of Kazakhstan. The major factors affecting the trend of area burned in Kazakhstan are wetter climate (represented as PDSI), the proportion of grassland cover, ANPP and livestock density (Table 2). Grassland enables spreading fires and ANPP enables sustaining fires.

The declining trends in the fraction of the area burned annually are shown in Fig. 5a. The trend of PDSI from March to July during the 15-year period is illustrated in Fig. 5b. A higher PDSI value indicates a wetter environment. Increasing wetness, i.e. higher PDSI, during the fire season reduces the probability of fire ignition and fire spread. The declining trend of the burned area (Fig. 5a) is then consistent of the increasing trend of PDSI (wet conditions) especially in central and southern Kazakhstan (e.g. East Kazakhstan, Qaraghandy, Zhambyl, Almaty) (Fig. 5b).

Through time the proportion of grassland cover has been asymmetric with some counties having exhibited strong decreases such as in the north central region of Kazakhstan, while others have seen increases such as in the north western region (Fig. 5c). This north central region has also exhibited decreases in burned area (Fig. 5a). Similarly, some regions have shown increasing trends of grassland cover through time without commensurate increases in the proportion of burned area (Figs. 5a and 5c).

The impacts of year, PDSI, grassland layer, ANPP and livestock density on the extent of the area burned and the correlations of burned area with these driving forces are illustrated in Fig. 6. Area burned and PDSI were negatively correlated in most of the counties in Kazakhstan (Fig. 6b). Therefore, as Kazakhstan becomes wetter during the fire season, the area burned declined over the 2002–2016 period. At the same time, grassland cover decreased across most of Kazakhstan, with a notable exception being the north central region and south western region (Fig. 6c). ANPP decreased with time over most of Kazakhstan, the exception being central and south western counites (Fig. 6d).

Finally, we investigated livestock density as a potential non-climatic driver affecting fuel amount. The population density of livestock increased with time in all counties and was greatest in the central, northern and southern counties of Qostanay, Pavlodar and Qaraghandy (Fig. 5e). The coupling of livestock density with PDSI affected the extent of the area burned (Fig. S1.4) with $p = 0.042$ (Table 2). The area burned was negatively correlated with the population of livestock throughout nearly all of Kazakhstan (Fig. 6e). This observation suggests the increasing population of grazing livestock may have reduced fuelbed continuity leading to the decrease of the area burned in Kazakhstan. Since 2000, the numbers of sheep, goats and cattle have increased by 60% in Kazakhstan based on MANE statistics (2019), respectively (Figs. S2 and S3). Thus, increased livestock grazing could decrease the amount of herbaceous fuel across the landscape and offset increases in fuel quantity due to expanded grassland cover. The net result would be reductions in fire spread and the area burned.

3.4 Interactions of driving forces

The driving forces (e.g. year, PDSI, proportion of grassland cover, ANPP, livestock density) for the decline of the burned areas in Kazakhstan from 2002 to 2016 are inter-related. It is therefore critical to evaluate their interactions. For instance, Figures S1.1–S1.4 illustrate the proportion of burned area is affected by the interactions of the driving forces at 174 counties over 15 years in Table 2.

Proportion of grassland cover and year Both year and the proportion of grassland area had significant effects on burned area when interacted (Table 2, $p < 0.001$). While the proportion of grassland cover in a county is very low (e.g. 0.48 %), only about 0.6 % of the area was burned annually during the period of the year 2002 to 2016 (Fig. S1.1, upper left panel). On the contrary, while the grassland cover is 25 %, the area burned declined steadily from 1.5 % in the year 2000 to 0.6 % in 2016 (Fig. S1.2 lower right panel). This observation is consistent with grassland enhancing the spread of fires in the absence of opposing factors.

PDSI and proportion of grassland area Both PDSI and the proportion of grassland area had significant effects on burned area when interacted (Table 2, $p = 0.028$). As in Fig. S1.2, for PDSI in a range of -4.5 to ~ 2, the percentage of the area burned remained about 0.6 % for grassland area of 0.5 % (upper left panel). On the other hand, when grassland cover of 60 %, the fraction of area burned declined from 2.2 % to 0.8 % (lower right panel). This analysis is consistent with grassland enhancing the spread of fires, as in the previous section of proportion of grassland cover through time, and illustrates that increasing wetness significantly decreases burned area mostly when grassland cover is high.

Livestock density and year We investigated livestock density as a potential non-climatic driver affecting fuel amount and area burned. The effects of grazing on the area burned during 2002 – 2016 are shown in Table 2, $p = 0{,}089$. The declining trend of the area burned with time for different livestock density are illustrated in Fig. S1.3. The higher the livestock density resulting in less available biomass to burn, the less area burned (lower right panel). It provides additional evidence that grazing could reduce the area burned in Kazakhstan.

PDSI and livestock density The interaction between PDSI and livestock was significant to affect the area burned ($p = 0.042$). Figure S1.4 shows the decline in the proportion of burned area with PDSI at different livestock densities. As PDSI increases (wetter landscape), less area is burned. However, the declining trends differ with livestock density. This relationship is quite different for the livestock density of 0.002 heads km^{-2} (Fig. S1.4 upper left panel) and 0.05 heads km^{-2} (Fig. S1,4 lower right panel). For instance, for low PDSI (-4, dry), 1.5 % of the area was burned for all livestock densities. On the contrary, at high PDSI (+2, wet), the percentage of burned area decreased with increasing livestock density. Thus, during dry years the area burned is unaffected by grazing intensity, but during wet years with high biomass (based on our RVS analysis of Reeves, 2016), high grazing intensity tends to decrease burned area.

4 Discussion

Burned area

The spatial and temporal extent of the area burned were examined in different ecosystems in northern Eurasia during 2002 to 2016, during which the average area burned was $(2.7 \pm 1.0) \times 10^5$ km^2 yr^{-1}. The burned area in grasslands declined 74 % from ~ 282,000 km^2 in 2002 to ~ 73,000 km^2 in 2016 at a rate of 1.3×10^4 km^2 yr^{-1}. The area burned in forest showed no trend over time. Our burned area is higher than the MODIS MCD64 collection 6, in which the average annual burned area was 9.7×10^4 km^2 in boreal Asia during the same period (Gigilio et al., 2018). Boreal Asia of MCD64 has a similar geographic region as our northern Eurasia. Nevertheless, the interannual variability and the trends of burned area for the two datasets are consistent (Fig. 3).

Our results on burned area trends are also consistent with other published results (Giglio et al., 2013; Hao et al., 2016a; Andela et al., 2017) that concluded the area burned in northern Eurasia declined, contrary to the projections of increased fire frequency driven by climate change (Groisman et al., 2007; Kharuk et al., 2008). Uncertainty in global burned area remains a critical challenge with high variability on trends and interannual variability between sensors and processing algorithms (Hantson et al., 2016; Chuvieco et al., 2019).

Grassland fires and grazing

Grassland fires in Kazakhstan accounted for 47 % of the total area burned but comprised 84 % of the decline of the total area burned in northern Eurasia during the 15 years of 2002–2016. The grassland fires are human caused to produce fresh grass for grazing (Lebed et al., 2012) with a cycle of about every two years. A similar temporal pattern characterizes grassland fire occurrence in the African savanna (Hao and Liu, 1994; Andela and van der Werf, 2014).

Central Asia experienced tremendous socioeconomic change, with the collapse of the Soviet Union in the 1990's leading to a full restructure of the agricultural system, followed by a rapid collapse of cattle industry and progressively recovered in the last 20 years, and potentially altering fuel availability to burn as observed in other ecosystems (Holdo et al. 2009, Vigan et al. 2017) (Figs. S2 and S3) (Food and Agriculture Organization, 2016; Robinson and Milner-Gulland, 2003). The coincident decline in burned area with increasing livestock population suggests changing agricultural practices may have exerted an influence on fire activity in Kazakhstan and northern Eurasia. In addition, the relationship between livestock population and the burned area was observed in arid grassland in a small region of southern Russia from 1986 to 2006 (Dubinin et al., 2011). During this time period, the livestock population was negatively correlated with the area burned.

The fire activity data for Kazakhstan and Mongolia can be estimated from1985 to 2017 as shown in Fig. 7 based on the recently released AHVRR long term fire history (Oton et al. 2019). This new information extends the analysis before our observed decrease during the 2002–2016 period and shows that fire activity increased in Kazakhstan just during the economic collapse and the associated reduction of livestock in the year 2000. This opposite trend supports our interpretation on the relationship between grazing and burned area, particularly when this variation in burned area is not clearly observed in neighboring Mongolia where grazing collapse did not occur.

In the steppe of neighboring Mongolia, overgrazing also affected fire activity from 1988–2008 (Liu et al., 2013) in a manner similar to Kazakhstan. However, extreme winter freezing and inadequate preparation affected the increasing livestock trend driven by the poorly prepared feeding of hay and foliage. It led to livestock reductions during the colder season than the average period during the years of 2000 to 2014 (Nandintsetseg et al. 2018), highlighting the potential impact of climate on livestock population beside human decisions and practices (Xu et al., 2019).

Modelling fire and grazing interactions

Accounting for confounding factors related to burned area and the subsequent effects on ecosystems, biosphere/atmosphere interactions and climate have been a challenge in developing fire modules in global vegetation models (Hantson et al. 2016). Climate (drought, temperature and humidity), land cover and fuel amount are the main drivers related to fire activity in Dynamic Global Vegetation Models (DGVMs) coupled with human-related information as population density. Obtaining data for simulating the dynamic of these human-related information remain a challenge. Major efforts have been devoted to understanding land use dynamic (Prestele et al. 2017), but forest management, fire prevention and grazing practices are still the major unknown requiring better data assemblage and modeling processes (Pongratz et al. 2018). In our study, we showed the strong impact of political events (here the collapse of the political regime) on grazing intensity and the subsequent effect on fire activity. These stochastic events are hard to forecast and simulate so that DGVM can capture long term trends in burned area (Yue et al. 2014, Kloster et al. 2010) when compared to observed burned area reconstructions (Mouillot and Field 2005).

The Russian economic collapse is unique to provide fruitful information on potential impact of grazing changes on ecosystem functioning when associated to socio-economic scenarios. Integrating grazing in DGVM has recently emerged for global models (Chang et al. 2013, Dangal et al. 2017, Pachzelt et al. 2015) and for local studies (Bachelet et al. 2000, Caracciolo et al. 2017, Vigan et al. 2017). Grazing processes can hardly capture both socio-economic scenarios and climate impact on livestock population which could be affected by climate extremes (Nandintsetseg et al. 2018) and lack of forage or water (Vrieling et al. 2016, Tachiiri and Shinoda 2012).

5 Conclusions

The spatial and temporal extent of the area burned were examined in different ecosystems in northern Eurasia from 2002 to 2016. We conclude

1) The burned area in grasslands declined 74 % from ~ 282,000 km^2 in 2002 to ~ 73,000 km^2 in 2016 or at a rate of 1.3×10^4 km^2 yr^{-1}. The area burned in forest did not show a trend.

2) Grassland fires in Kazakhstan accounted for 47 % of the total area burned but comprised 84 % of the decline of the total area burned in northern Eurasia during the 15 years.
3) Wetter climate and the increase of grazing livestock in Kazakhstan are the major factors contributing to the decline of the area burned in northern Eurasia.
4) Most of Kazakhstan became wetter from 2002 to 2016, decreasing high fire years due to less frequent dry years.
5) The population of livestock increased in most of Kazakhstan from 2002 to 2016, decreasing the burned area during the wettest years by fuel removal from grazing.
6) The major factors affecting the availability of the fuels for the decline of burned area are: climate, proportion of the grassland cover, aboveground net primary production and livestock density. These factors interact to reduce the area burned in Kazakhstan, especially in grassland.

Data availability. All data and materials are available in the manuscript or the supplementary materials. The original geospatial dataset of the burned area is large and will be available upon reasonable request. However, a derived dataset has been used to estimate black carbon emissions from fires in the same region. It has been archived at the Forest Service Data Archive web site (Hao et al., 2016b). https://www.fs.usda.gov/rds/archive/Product/RDS-2016-0036/

*Supplemen*t. The supplement for this article is available online at: xxx.

Author contributions. W.M.H. led the project and led writing the manuscript. M.C.R. simulated aboveground biomass ANPP and advised statistical analysis. L.S.B. was responsible for statistical analysis. Y.B., P.C. and F.M. suggested the use of PDSI and livestock population to explain the declining burned areas. B.N. analyzed the data and contributed certain figures. A.P. mapped burned areas., R.E.C. conducted GIS analysis. S.P.U. advised the execution of the project. C.Y. advised on the trend of the burned areas. All authors contributed the writing of the manuscript

Competing interests. The authors do not have competing interests.

Acknowledgements. W.M.H. received funding from the US Department of State, US Forest Service Research and Development, and NASA Terrestrial Ecology Program. Y.B. and P.C. have received funding from the European Union's Horizon 2020 research and innovation program under grant agreement No 641816 (CRESCENDO). F.M. received funding from ESA FIRECCI program.

References

Abatzoglou, J. T. and Kolden, C. A.: Relationships between climate and macroscale area burned in the western United States, International Journal of Wildland Fire, 22, 1003–1020, http://dx.doi.org/10.1071/WF13019, 2013.

Andela, N. and van der Werf, G. R.: Recent trends in African fires driven by cropland expansion and El Niño to La Niña transition, Nature Climate Change, 4, 791-795, https://doi: 10.1038/NCLIMATE2313., 2014.

Andela, N., Morton, D. C., Giglio, L., Chen, Y., van der Werf, G. R., Kasibhatla, P. S., DeFries, R. S., Collatz, G. J., Hantson, S., Kloster, S., Bachelet, D., Forrest, M., Lasslop, G., Li, F., Mangeon, S., Melton, J. R., Yue, C., and Randerson, J. T.: A human-driven decline in global burned area, Science, 356, 1356-1362, https:// doi: 10.1126/science.aal4108, 2017.

Archibald, S., Roy, D. P., van Wilgen, B. W., and Scholes, R. J.: What limits fire? An examination of drivers of burnt area in Southern Africa, Global Change Biology, 15, 613-630, doi:10.1111/j.1365-2486.2008.01754.x, 2009.

Bachelet, D., Lenihan, J. M., Daly, C., and Neilson, R. P.: Interactions between fire, grazing and climate change at Wind Cave National Park, SD, Ecological Modelling, 134, 229–244, https://doi.org/10.1016/j.rama.2015.10.011, 2000.

Brooks, M. E., Kristensen, K., van Benthem, K. J., Magnusson, A., Berg, C. W., Nielsen, A., Skaug, H. J., Machler, M. and Bolker, B. M.: glmmTMB balances speed and flexibility among packages for zero-inflated generalized linear mixed modeling, The R Journal, 9(2), 378-400, 2017.

Caracciolo, D., Istanbulluoglu, E., and Noto, L.V.: An ecohydrological cellular automata model investigation of juniper tree encroachment in a western north American landscape, Ecosystems, 20, 1104-1123, https://doi.org/10.1007/s10021-016-0096-6, 2017

Cowtan, K. and Way, R. G.: Coverage bias in the HadCRUT4 temperature series and its impact on recent temperature trends, Q. J. R. Meteorol. Soc, 140, 1935-1944, https://doi.org/10.1002/qj.2297, 2014.

Chang, J. F., Viovy, N., Vuichard, N., Ciais, P., Wang, T., Cozic, A., Lardy, R., Graux, A.-L, Klumpp, K., Martin, R., and Soussana, J. F.: Incorporating grassland management in ORCGIDEE: model description and evaluation at 11 eddy-covariance sites in Europe, Geosci. Model Dev., 6, 2165-2181, https://doi.org/10.5194/gmd-6-2165-2013, 2013.

Chuvieco, E., Mouillot, F., van der Werf, G. R., San Miguel, J., Tanase, M., Koutsias, N., García, M., Yebra, M., Padilla, M., Gitas, I., Heil, A., Hawbaker, T. J., and Giglio, L.: Historical background and current developments for mapping burned area from satellite Earth observation, Remote Sens. Environ., 225, 45-64, https://doi.org/10.1016/j.rse.2019.02.013, 2019.

Dangal, S. R. S., Tian, H., Lu, C., Ren, W., Pan, S., Yang, J., Di Cosmo, N., and Hessl, A.: Integrating herbivore population dynamics into a global land biosphere model: plugging animals into the earth system, Journal of advances in modeling earth systems, 9, 2920-2945, https://doi.org/10.1002/2016MS000904, 2017.

Dubinin, M., Luschekina, A., and Radeloff, V. C.: Climate, livestock, and vegetation: what drives fire increase in the arid ecosystems of southern Russia? Ecosystems, 14, 547-562, https://doi: 10.1007/s10021-011-9427-9, 2011.

Evangeliou, N., Balkanski, Y., Hao, W. M., Petkov, A., Silverstein, R. P., Corley, R., Nordgren, B. L., Urbanski, S. P., Eckhardt, S., Stohl, A., Tunved, P., Crepinsek, S., Jefferson, A., Sharma, S., Nøjgaard, J. K., and Skov, H.: Wildfires in northern Eurasia affect the budget of black carbon in the Arctic – a 12-year retrospective synopsis (2002–2013), Atmos. Chem. Phys., 16, 7587-7604, https://doi.org/10.5194/acp-16-7587-2016, 2016.

Food and Agriculture Organization FAOSTAT Live Animals Database, http://www.fao.org/faostat/en/#home, 2016.

Friedl, M. A., Sulla-Menashe, D., Tan, B., Schneider, A., Ramankutty, N., Sibley, A., and Huang, X.: MODIS collection 5 global land cover: algorithm refinements and characterization of new datasets, Remote Sens. Environ., 114, 168-182, https://doi.org/10.1016/j.rse.2009.08.016, 2010.

Fyfe, J. C., Gillett, N. P., and Zwiers, F. W.: Overestimated global warming over the past 20 years. Nature Clim Chang, 3, 767-769, https://doi.org/10.1038/nclimate1972, 2013.

Gedalof, Z., Peterson, D. L., and Mantua, N. J.: Atmospheric, climatic, and ecological controls on extreme wildfire years in the northwestern United States, Ecological Applications, 15, 154–174, https://doi.org/10.1890/03-5116, 2005.

Giglio, L., Boschetti, L., Roy, D., Humber, M. L., and Justice, C. O.: The collection 6 MODIS burned are mapping algorithm and product, Remote Sens. Environ., 217, 72-85, https://doi.org/10.1016/j.rse.2018.08.005, 2018.

Giglio, L., Randerson, J. T., and van der Werf, G. R.: Analysis of daily, monthly, and annual burned area using the fourth-generation global fire emissions database (GFED4), J. Geophys. Res. Biogeosci., 118, 317–328, doi:10.1002/jgrg.20042, 2013.

Goetz, S. J., MacK, M. C., Gurney, K. R., Randerson, J. T., and Houghton, R. A.: Ecosystem responses to recent climate change and fire disturbance at northern high latitudes: observations and model results contrasting northern Eurasia and North America, Environ. Res. Lett., 2, 045031, https://doi.org/10.1088/1748-9326/2/4/045031, 2007.

Goldammer, J. G., Stocks, B. J., Sukhinin, A. I., and Ponomarev, E.: Current fire regimes, impacts and likely challenges - II: forest fires in Russia - past and current trends. in Vegetation Fires and Global Change, Goldammer, J. G., Ed., 51-78, 2013.

Groisman, P. Ya., Sherstyukov, B. G., Razuvaev, V. N., Knight, R. W., Enloe, J. G., Stroumentova, N. S., Whitfield, P. H., Førland, E., Hannsen-Bauer, I., Tuomenvirta, H., Aleksandersson, H., Mescherskaya, A. V., and Karl, T. R.: Potential forest fire danger over Northern Eurasia: Changes during the 20th century, Global and Planetary Change, 56, 371-386, https://doi.org/10.1016/j.gloplacha.2006.07.029, 2007.

Hantson, S., Arneth, A., Harrison, S. P., Kelley, D. I., Prentice, I. C., Rabin, S. S., Archibald, S., Mouillot, F., Arnold, S. R., Artaxo, P., Bachelet, D., Ciais, P., Forrest, M., Friedlingstein, P., Hickler, T., Kaplan, J. O., Kloster, S., Knorr, W., Lasslop, G., Li, F., Mangeon, S., Melton, J. R., Meyn, A., Sitch, S., Spessa, A., van der Werf, G. R., Voulgarakis, A., and Yue, C.: The status and challenge of global fire modelling, Biogeosciences, 13, 3359-3375, DOI: 10.5194/bg-13-3359-2016, 2016.

Hao, W. M. and Liu, M.-H.: Spatial and temporal distribution of tropical biomass burning, Global Biogeochem. Cy., 8, 495-503, https://doi.org/10.1029/94GB02086, 1994.

Hao, W. M., Petkov, A., Nordgren, B. L., Corley, R. E., Silverstein, R. P., Urbanski, S. P., Evangeliou, N., Balkanski, Y., and Kinder, B. L.: Daily black carbon emissions from fires in northern Eurasia for 2002–2015, Geosci. Model Dev., 9, 4461-4474, www.geosci-model-dev.net/9/4461/2016/doi:10.5194/gmd-9-4461-2016, 2016a.

Hao, W. M., Petkov, A., Nordgren, B. L., Corley, R. E., Silverstein, R. P., and Urbanski, S. P.: Daily black carbon emissions data from fires in Northern Eurasia for 2002–2015, Forest Service Research Data Archive, https://doi.org/10.2737/RDS-2016-0036, 2016b.

Holdo, R. M., Holt, R. D., and Fryxell, J. M.: Grazers, browsers, and fire influence the extent and spatial pattern of tree cover in the Serengeti, Ecological Applications, 19, 95-109, https://doi.org/10.1890/07-1954.1, 2009.

Huber, P. J.: Statistics, John Wiley& Sons, 1981.

IPCC, 2013: Climate Change 2013: The Physical Science Basis. Contribution of Working Group I to the Fifth Assessment Report of the Intergovernmental Panel on Climate Change [Stocker, T.F., D. Qin, G.-K. Plattner, M. Tignor, S.K. Allen, J. Boschung, A. Nauels, Y. Xia, V. Bex and P.M. Midgley (eds.)]. Cambridge University Press, Cambridge, United Kingdom and New York, NY, USA, 1535 pp., 2013.

IPCC, 2014: Climate Change 2014: Synthesis Report. Contribution of Working Groups I, II and III to the Fifth Assessment Report of the Intergovernmental Panel on Climate Change [Core Writing Team, R.K. Pachauri and L.A. Meyer (eds.)]. IPCC, Geneva, Switzerland, 151 pp., 2014.

Jolly, W. M., Cochrane, M. A., Freeborn, P. H., Holden, Z. A., Brown, T. J., Williamson, G. J., and Bowman, D. M. J. S.: Climate-induced variations in global wildfire danger from 1979 to 2013, Nature communications, 6, 7537, https://doi.org/10.1038/ncomms8537, 2015.

Kendall, M.: A new measure of rank correlation, Biometrika. 30 (1–2): 81–89, 1938.

Kharuk, V. I., Ranson, K. J., and Dvinskaya, M. L.: Wildfire dynamics in larch dominance zone, Geophys, Res. Lett., 35, L01402, https://doi.org/10.1029/2007GL032291, 2008.

Kloster, S., Mahowald, N. M., Randerson, J. T., Thornton, P. E., Hoffman, F. M., Levis, S., Lawrence, P. J., Feddema, J. J., Oleson, K. W., and Lawrence, D. M.: Fire dynamics during the 20th century simulated by the community land model, Biogeosciences, 7, 1877-1902, https://doi.org/10.5194/bg-7-1877-2010, 2010.

Koerner, S. E. and Collins, S. L.: Interactive effects of grazing, drought, and fire on grassland plant communities in North America and South Africa, Ecology, 95, 98–109, https://doi.org/10.1890/13-0526.1, 2014.

Krawchuck, M. A. and Moritz, M. A.: Constraints on global fire activity vary across a resource gradient, Ecology, 92, 121-132, https://doi.org/10.1890/09-1843.1, 2011.

Liu, Yi. Y., Evans, J. P., McCabe, M. F., de Jeu, R. A. M., van Dijk, A. I. J. M., Dolman, A. J., and Saizen, I.: Changing climate and overgrazing are decimating Mongolian steppes, PLoS ONE 8, e57599, https://doi.org/10.1371/journal.pone.0057599, 2013.

MANE: National Economy of the Republic of Kazakhstan Committee on Statistics. 2019. http://www.stat.gov.kz/faces/wcnav_externalId/homeNumbersAgriculture. Last Visited April 28, 2019.

Mondal, N. and Sukumar, R.: Fires in seasonally dry tropical forest: testing the varying constraints hypothesis across a regional rainfall gradient, PLoS ONE, 11, e0159691, https://doi.org/10.1371/journal.pone.0159691, 2016.

Moritz, M. A., Morais, M. E., Summerell, L. A., Carlson, J. M., and Doyle, J.: Wildfires, complexity, and highly optimized tolerance, PNAS, 102, 17912-17917, https://doi.org/10.1073/pnas.0508985102, 2005.

Mouillot, F. and Field, C. B.: Fire history and the global carbon budget: a 1° x 1° fire history reconstruction for the 20th century, Global Change Biology, 11, 398-420, https://doi.org/10.1111/j.1365-2486.2005.00920.x, 2005.

Mouillot, F., Schultz, M. G., Yue, C., Cadule, P., Tansey, K., Ciais, P., and Chuvieco, E.: Ten years of global burned area products from spaceborne remote sensing - a review: analysis of user needs and recommendations for future developments, International Journal of Applied Earth Observation and Geoinformation, 2014, 26, 64-79, https://doi.org/10.1016/j.jag.2013.05.014, 2014.

Nandintsetseg, B., Shinoda, M., Du, C., and Munkhjargal, E: Cold-season disasters on the Eurasian steppes: climate-driven or man-made, Scientific reports, 8, 15905, https://doi.org/10.1038/s41598-018-33046-1, 2018.

NASA Global Climate Change, https://climate.nasa.gov/vital-signs/global-temperature/, last access, September 12, 2019.
Official Agriculture Statistics of Kazakhstan, http://www.stat.gov.kz/faces/wcnav_externalId/homeNumbersAgriculture, 2016.
Otón, G., Ramo, R., Lizundia-Loiola, J., and Chuvieco, E.: Global detection of long-term (1982–2017) burned area with AVHRR-LTDR data, Remote Sens., 11, 2079, https://doi.org/10.3390/rs11182079, 2019.
Pachzelt, A., Forrest, M., Ramming, A., Higgins, S. I, and Hickler, T.: Potential impact of large ungulate grazers on African vegetation, carbon storage and fire regimes, Global ecology and biogeography, 24, 991-1002, https://doi.org/10.1111/geb.12313, 2015.
Palmer, W., Meteorological drought, U.S. Department of Commerce, Weather Bureau, Research Paper, 45, 1965.
Pausas, J. G. and Ribeiro, E.: The global fire-productivity relationship, Global ecology and biogeography, 22, 728-736, https://doi.org/10.1111/geb.12043, 2013.
Pongratz, J., Dolman, H., Don, A., Erb, K.-H., Fuchs, R., Herold, M., Jones, C., Kuemmerle, T., Luyssaert, S., Meyfroidt, P., and Naudts, K.: Models meet data: Challenges and opportunities in implementing land management in earth system models. Global change biology, 24, 1470-1487, https://doi.org/10.1111/gcb.13988, 2018.
Prestele, R., Arneth, A., Bondeau, A., De Noblet-Ducoudre, N., Pugh, T. A. M., Sitch, S., Stehfest, E., and Verburg, P. H.: Current challenges of implementing anthropogenic land-use and land-cover change in models contributing to climate change assessments, Earth system dynamics, 8, 369-386, doi:10.5194/esd-8-369-2017, 2017.
R Core Team: R: A language and environment for statistical computing. R Foundation for Statistical Computing, Vienna, Austria. URL https://www.R-project.org/, 2019.
Reeves, M. C.: Development of the rangeland vegetation simulator: A module of the forest vegetation simulator. Final report to the Joint Fire Science Program, Boise, Idaho, 2016.
Riley, K. L., Abatzoglou, J. T., Grenfell, I. C., Klene, A. E., and Heinsch, F. A.: The relationship of large fire occurrence with drought and fire danger indices in the western USA, 1984–2008, International Journal of Wildland Fire, 22, 894–909, https://doi.org/10.1071/WF12149, 2013.
Robinson, S. and Milner-Gulland, E. J.: Political change and factors limiting numbers of wild and domestic ungulates in Kazakhstan, Human Ecology, 31, 87-110, https://doi.org/10.1023/A:1022834224257, 2003.
Roy, D. P., Boschetti, L., Justice, C.O., and Ju, J.: The collection 5 MODIS burned area product – global evaluation by comparison with the MODIS active fire product, Remote Sens. Environ., 112, 3690-3707, https://doi.org/10.1016/j.rse.2008.05.013, 2008.
Scheiter, S. and Savadogo, P.: Ecosystem management can mitigate vegetation shifts induced by climate change in West Africa, Ecological Modelling, 332, 19-27, https://doi.org/10.1016/j.ecolmodel.2016.03.022, 2016.
Seneviratne, S. I, Donat, M. G., Mueller, B., and Alexander, L.V.: No pause in the increase of hot temperature extremes, Nature Climate Change, 4, 161-163, https://doi.org/10.1038/nclimate2206, 2014.
Tachiiri, K and Shinoda, M.: Quantitative risk assessment for future meteorological disasters reduced livestock mortality in Mongolia, Climatic Change, 113, 867-882, https://doi.org/10.1007/s10584-011-0365-5, 2012.

Trenberth, K. E., Fasullo, J. T., Branstator, G., and Phillips, A. S.: Seasonal aspects of the recent pause in surface warming, Nature Climate Change, 4, 911-916, https://doi.org/10.1038/nclimate2341, 2014.

Trendberth, K. E., Fasullo, J. T., and Shepherd, T. G.: Attribution of climate extreme events, Nature Climate Change, 5, 725-730, https://doi.org/10.1038/nclimate2657, 2015.

Vandergert, P. and Newell, J. P.: Illegal logging in the Russian Far East and Siberia, Int. For. Rev., 5, 303-306, https://doi.org/10.1505/IFOR.5.3.303.19150, 2003.

Venables W. N. and Ripley, B. D.: Modern Applied Statistics with S, Fourth edition. Springer, New York. ISBN 0-387-95457-0, 2002.

Vigan, A., Lasseur, J., Benoit, M., Mouillot, F., Eugéne, M., Mansard, L., Vigne, M., Lecomte, P., and Dutilly, C.: Evaluating livestock mobility as a strategy for climate change mitigation: combining models to address the specificities of pastoral systems, Agriculture Ecosystems and Environment, 242, 89-101, https://doi.org/10.1016/j.agee.2017.03.020, 2017.

Vrieling, A., Meroni, M., Mude, A. G., Chantarat, S., Ummenhofer, C. C., and de Bie, K.: Early assessment of seasonal forage availability for mitigating the impact of drought on East African pastoralists, Remote Sens. Environ., 174, 44-55, https://doi.org/10.1016/j.rse.2015.12.003, 2016.

Xu, Y., Zhang, Y., Chen, J., and Ranjeet, J.: Livestock dynamics under changing economy and climate in Mongolia, Land Use Policy, 88, 104120, https://doi.org/10.1016/j.landusepol.2019.104120, 2019.

Yue, C., Ciais, P., Cadule, P., Thonicke, K., Archibald, S., Poulter, B., Hao, W. M., Hantson, S., Mouillot, F., Friedlingstein, P., Maignan, F., and Viovy, N.: Modelling the role of fires in the terrestrial carbon balance by incorporating SPITFIRE into the global vegetation model ORCHIDEE- part 1: simulating historical global burned area and fire regimes. Geosci. Model Dev., 7, 2747-2767, https://doi.org/10.5194/gmd-7-2747-2014, 2014.

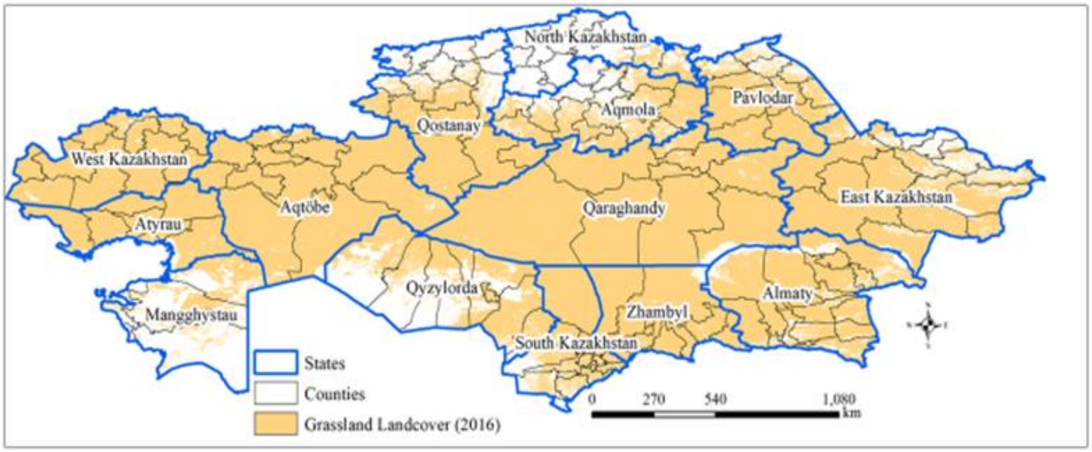

Figure 1. The distribution of grassland cover in Kazakhstan with counties and states shown as administrative boundaries.

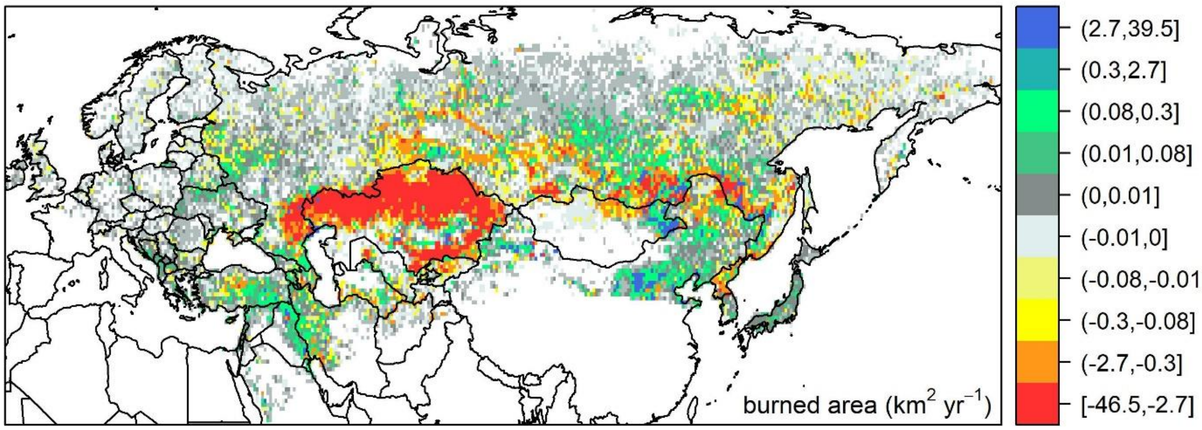

Figure 2. Spatial distributions of robust linear trends of the area burned for each 0.5° × 0.5° grid cell in northern Eurasia from 2002 to 2016.

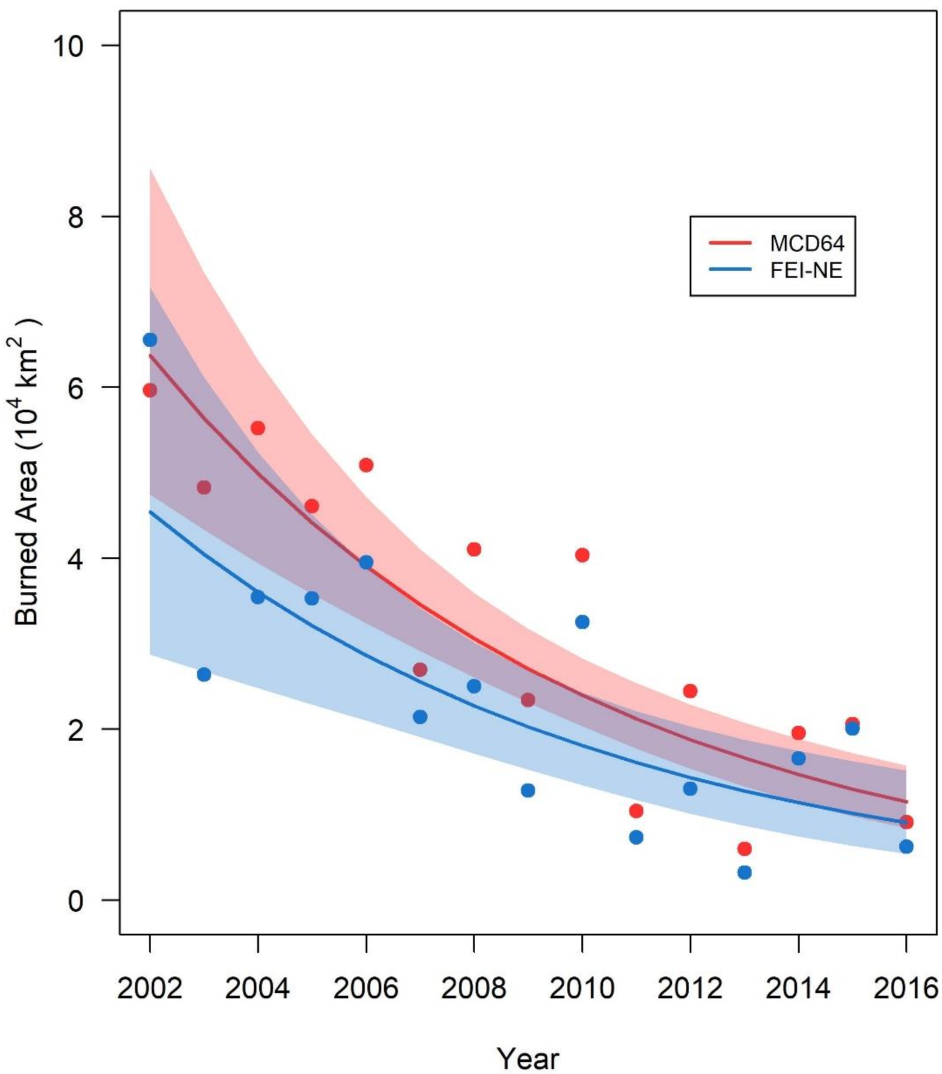

Figure 3. Comparison of burned areas between the dataset of Forest Service Fire Emission Inventory – northern Eurasia (FEI-NE) and MODIS MCD64. The FEI-NE (blue) and MCD64 (pink) bands illustrate the 95% confidence intervals.

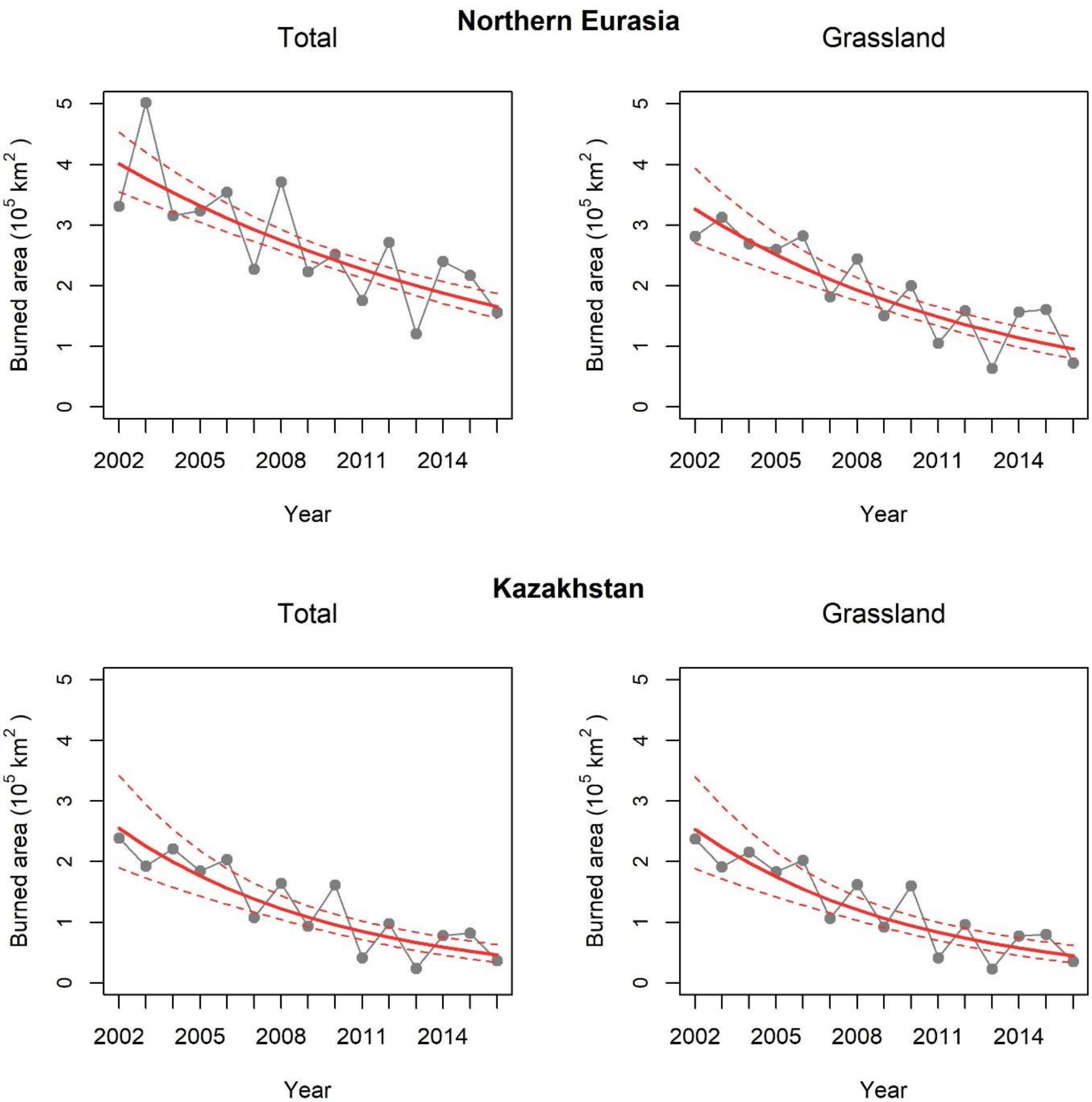

Figure 4. Declining trends of the total area and grassland area burned in northern Eurasia and Kazakhstan from 2002 to 2016. The solid lines are the trend lines and the dotted lines are 95% confidence intervals.

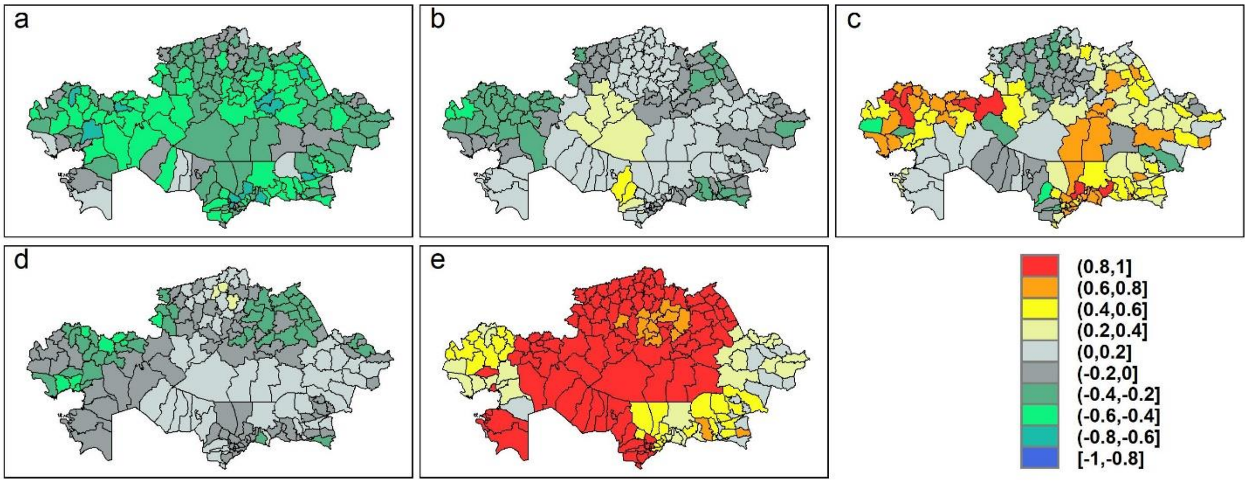

Figure 5. Pairwise robust rank correlations of year with (**a**) fraction of burned area, (**b**) PDSI, (**c**) proportion of grassland layer, (**d**) ANPP and (**e**) livestock density without considering their interactions.

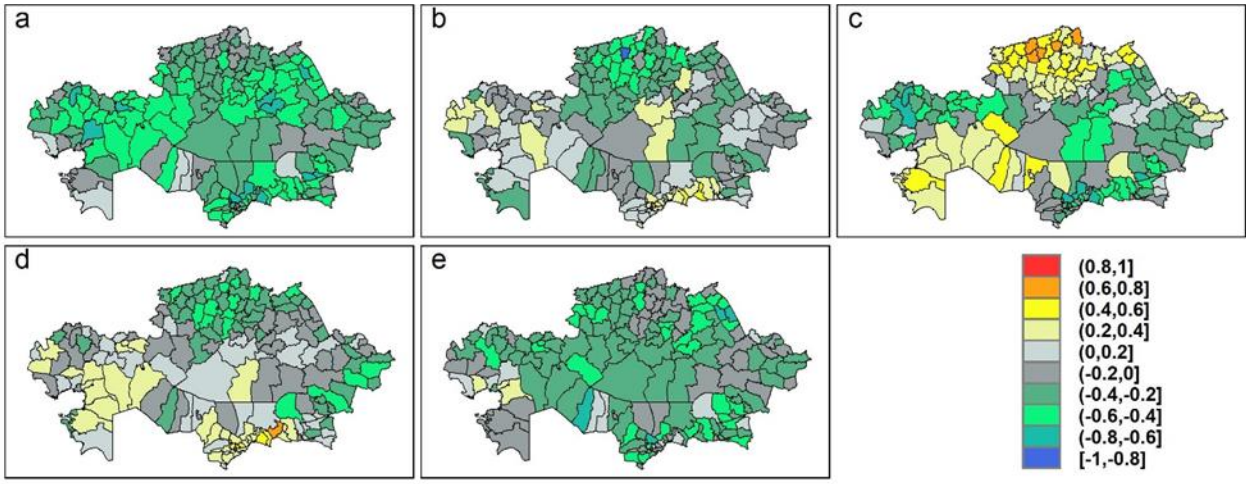

Figure 6. Pairwise robust rank correlations of fraction of burned area with (**a**) year, (**b**) PDSI, (**c**) proportion of grassland layer, (**d**) ANPP and (**e**) livestock density without considering their interactions.

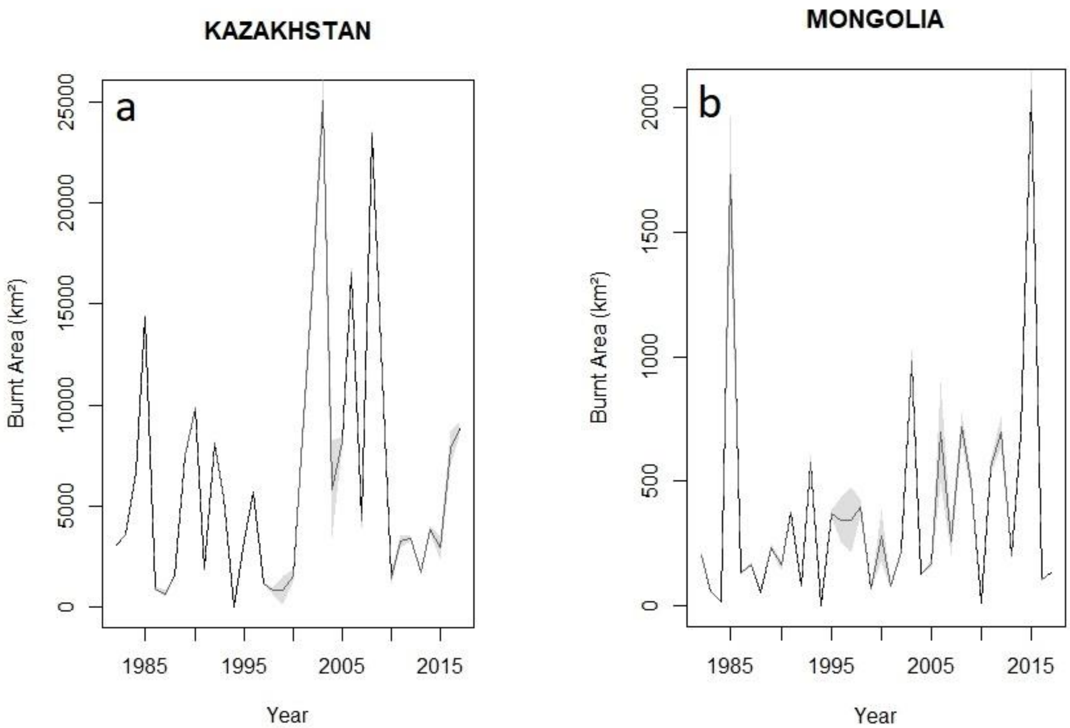

Figure 7. Yearly burned area (in km2) in (**a**) Kazakstan and (**b**) Mongolia for the 1982-2017 periode based on the AVHRR remotely sensed burned area **L**ong Term **D**ata **R**ecord_Climatte Change Initiative (FIRECCILT10) (https://www.mdpi.com/2072-4292/11/18/2079, Otón et al., 2019). Black line represents mean burned fraction and grey area the burned area 95% uncertainty delivered by FIRECCILT10

Table 1. The area burned in forest, grassland, shrubland and savanna in geographic regions from 2002 to 2016. The data of the area burned in Kazakhstan are listed for comparison only, and are not included in the tabulation.

	Burned Area (km^2)															
Region	**2002**	**2003**	**2004**	**2005**	**2006**	**2007**	**2008**	**2009**	**2010**	**2011**	**2012**	**2013**	**2014**	**2015**	**2016**	**Total**
Forest (Evergreen Needleleaf, Evergreen Broadleaf, Deciduous Needleleaf, Deciduous Broadleaf, Mixed)																
Russia	26,458	99,944	16,715	20,561	32,929	23,731	72,671	33,356	19,309	43,910	73,920	29,791	62,701	38,511	51,718	646,223
East Asia	1,483	9,697	6,368	4,202	2,814	2,524	4,597	6,676	1,258	3,379	4,189	1,819	3,151	2,944	1,336	56,436
Central & Western Asia	131	206	367	259	388	469	641	389	348	159	321	307	517	726	455	5,684
Europe	376	1,172	467	592	491	1,170	850	863	328	1,206	2,307	537	1,224	1,756	575	13,911
Subtotal	28,448	111,019	23,917	25,613	36,623	27,894	78,758	41,283	21,243	48,653	80,736	32,455	67,592	43,937	54,084	722,254
Grassland																
Russia	32,019	97,754	33,372	61,755	62,973	55,220	65,144	46,375	30,634	43,760	37,261	21,114	51,745	49,857	22,178	711,160
East Asia	10,643	21,235	15,551	12,433	14,456	16,819	15,278	11,259	8,097	18,716	23,870	18,123	26,689	29,361	13,962	256,492
Central & Western Asia	239,160	193,580	220,080	185,531	204,627	109,248	163,814	92,592	161,668	41,943	97,363	24,364	78,203	81,517	36,369	1,930,057
Europe	128	271	108	555	241	616	325	217	104	401	526	150	186	237	179	4,242
Subtotal	281,948	312,840	269,112	260,273	282,296	181,903	244,560	150,443	200,503	104,819	159,021	63,752	156,822	160,972	72,688	2,901,951
Kazakhstan	237,335	191,466	215,977	182,968	202,292	106,558	162,474	91,873	160,318	40,995	96,420	23,195	76,977	80,251	35,249	1,904,348
Shrubland (Closed Shrubland and Open Shrubland)																
Russia	7,042	27,749	4,894	13,149	5,924	2,868	10,901	13,096	18,854	6,697	12,650	10,918	5,717	3,486	14,529	158,470
East Asia	337	79	264	828	934	675	790	645	375	914	796	193	317	153	191	7,490
Central & Western Asia	1,022	2,836	5,632	2,384	1,255	1,728	999	1,217	3,279	964	769	845	1,066	1,287	1,720	27,001
Europe	20	38	23	70	39	121	112	87	21	83	70	11	13	10	17	732
Subtotal	8,421	30,701	10,813	16,430	8,152	5,391	12,802	15,044	22,529	8,657	14,285	11,966	7,112	4,934	16,457	193,693
Savanna (Woody Savanna and Savanna)																
Russia	11,136	43,574	8,307	19,343	25,129	10,465	33,347	14,191	6,745	12,473	16,387	12,076	8,324	6,261	12,039	239,796
East Asia	589	3,504	3,257	1,275	1,564	694	1,268	1,349	465	611	660	205	147	510	131	16,226
Central & Western Asia	575	500	437	395	442	317	413	391	261	115	193	112	161	301	178	4,791
Europe	83	207	110	293	200	653	340	400	113	319	426	212	201	142	243	3,941
Subtotal	12,383	47,785	12,110	21,306	27,335	12,128	35,368	16,330	7,584	13,517	17,666	12,604	8,832	7,215	12,592	264,753
Total	331,199	502,346	315,951	323,621	354,405	227,317	371,488	223,100	251,859	175,646	271,707	120,777	240,358	217,058	155,820	4,082,650

Table 2. Model parameters and associated *p*-values.

Parameter	*Estimate*	*Std. Error*	*z*	*Pr(>|z|)*
Year * ANPP	-0.02	0.01	-4.03	<0.001
Year * PDSI	0.00	0.00	0.20	0.838
Year * Proportion Grass Area	-0.26	0.04	-6.77	<0.001
Year * Livestock Density (head km^{-2})	1.04	0.61	1.70	0.089
ANPP * PDSI	-0.01	0.01	-0.92	0.360
ANPP * Proportion Grass Area	0.72	0.19	3.83	<0.001
ANPP * Livestock Density (head km^{-2})	0.88	3.22	0.27	0.784
PDSI * Proportion Grass Area	-0.24	0.11	-2.20	0.028
PDSI * Livestock Density (head km^{-2})	-3.30	1.62	-2.04	0.042
Proportion Grass Area * Livestock Density (head km^{-2})	37.78	28.32	1.33	0.182

Estimate = parameter estimate from GLMM, Std. Error = standard error of parameter estimate, z = z-statistic, Pr(>|z|) = p-value.